TISSUE ENGINEERING: Part A
Volume 22, Numbers 7 and 8, 2016

DOI: 10.1089/ten.tea.2015.0310

termis
Tissue Engineering
& Regenerative Medicine
International Society

ORIGINAL ARTICLE

Oxygen Tension-Controlled Matrices with Osteogenic and Vasculogenic Cells for Vascularized Bone Regeneration *In Vivo*

Ami R. Amini, DMD, PhD,[1,2] Thomas O. Xu,[2,3]
Ramaswamy M. Chidambaram, DVM, PhD,[4] and Syam P. Nukavarapu, PhD[2,3,5,6]

Despite recent progress, segmental bone defect repair is still a significant challenge in orthopedic surgery. While bone tissue engineering approaches using biodegradable matrices along with bone/blood vessel forming cells offered improved possibilities, current regenerative strategies lack the ability to achieve vascularized bone regeneration in critical-sized/segmental bone defects. In this study, we introduced and evaluated a two-pronged approach for vascularized bone regeneration *in vivo*. The goal was to demonstrate vascularized bone formation using oxygen tension-controlled (OTC) matrices seeded with bone and blood vessel forming cells. OTC matrices were coimplanted with rabbit mesenchymal stem cells (MSCs) and peripheral blood-derived endothelial progenitor cells (PB-EPCs) to demonstrate the osteogenic and vasculogenic differentiation of these cells, postseeding on a matrix, especially deep inside the matrix pore structure. Matrices coimplanted with varied rabbit MSC and PB-EPC ratios (1:4, 1:1, and 4:1) were assessed in a nude mouse subcutaneous implantation model to determine a coimplantation ratio with superior osteogenic as well as vasculogenic properties. The implants were analyzed, at week 8, for endothelial (CD31 and Von Willebrand factor [vWF]) and osteogenic marker (RunX2 and Col I) staining qualitatively and collagen deposition and number of vessel formation quantitatively. Results from these experiments established MSC-to-PB-EPC ratio 1:1 as the best coimplantation ratio. OTC matrix with 1:1 coimplantation ratio was assessed for segmental bone defect repair in a rabbit critical-sized bone defect model. The group under investigation was OTC matrix, and the matrix was seeded with MSCs, EPCs, or MSCs:EPCs in a 1:1 ratio. Explants at week 12 were evaluated for bone defect repair via micro-CT and histology. Results from rabbit *in vivo* experiments show enhanced mineralization and vascularization for the 1:1 coimplantation group. Overall, the study establishes a two-pronged approach involving OTC matrix and effective progenitors for large-area and vascularized bone regeneration.

Introduction

Vascularized bone regeneration is a significant challenge in bone tissue engineering.[1–5] Lack of vascularization often results in surface-limited bone regeneration *in vitro* as well as *in vivo*.[6–8] There is a growing need to develop tissue engineering strategies for bone regeneration throughout the graft (i.e., large-area bone regeneration) via graft vascularization, and such methods are potentially applicable for segmental and critical-sized bone defect repair.[9–13]

Many cellular-based bone tissue engineering approaches involve the use of bone marrow-derived mesenchymal stem cells (MSCs) as osteoprogenitor cells to promote and accelerate bone regeneration.[2,14,15] In this approach, MSCs are seeded on scaffolds for colonization and implantation at a defect site.[16,17] However, upon implantation, colonized cells in the interior regions of scaffolds with depth dimensions greater than 1 mm experience limited oxygen and nutrient availability since they are dependent on post-implantation vascularization that may occur on the order of days to weeks.[1,18] Due to limited nutrient delivery and waste product removal via diffusion, proper functional vascularization, cell viability, in turn, bone regeneration, and host integration are severely hindered.[7,19]

[1]Oral and Maxillofacial Surgery, Massachusetts General Hospital, Boston, Massachusetts.
[2]Institute for Regenerative Engineering, University of Connecticut Health Center, Farmington, Connecticut.
[3]Department of Orthopedic Surgery, University of Connecticut Health Center, Farmington, Connecticut.
[4]Center for Comparative Medicine, University of Connecticut Health Center, Farmington, Connecticut.
Departments of [5]Materials Science & Engineering, [6]Biomedical Engineering, University of Connecticut, Storrs, Connecticut.

Efficient methods to establish near-immediate neovascularization in bone tissue-engineered constructs are essential.[20] *In vitro* prevascularization of bone tissue engineering constructs with endothelial progenitor cells (EPCs) has gained significant attention in this respect.[21–26] EPCs, which may be easily isolated from the patient's peripheral blood, demonstrate high proliferative potential for *ex vivo* expansion, as well as the ability to enhance and accelerate neovascularization *in vivo*.[27] Moreover, when coimplanted with MSCs at a bone defect site, enhanced neovascularization and bone formation are observed. This enhancement is a result of synergistic communication (i.e., ''crosstalk'') between MSCs and EPCs,[28,29] where MSCs have been shown to release angiogenic factor vascular endothelial growth factor (VEGF),[30,31] and EPCs have been shown to release osteogenic factor, such as BMP-2 and BMP-4.[32,33] Although this prevascularization approach with EPC and MSC combination has been examined before, the effective cell ratio along with a TE matrix for long-bone defect repair has not been investigated. Our study aims to investigate optimum cocultures of rabbit peripheral bone marrow-derived MSCs and rabbit peripheral blood-derived EPCs (PB-EPCs) *in vivo* for vascularized bone regeneration.

Since bone formation requires a matrix that supports cell survival until the graft is vascularized as well as a cell combination that promotes osteogenesis and vasculogenesis, we propose a two-pronged approach for vascularized bone formation *in vivo*. Bone regeneration with either optimal matrix or efficient cell combination has been achieved,[12,24,34,35] but we hypothesize that large-area and vascularized bone regeneration is only possible by adopting the two-pronged approach. Our group has previously established oxygen tension-controlled (OTC) matrices that demonstrated enhanced performance, specifically with respect to increased oxygen tension levels, near-normal pH levels, and increased cell viability in the interior regions of the constructs after long-term *in vitro* culture with MSCs and EPCs.[35,36] This study is designed to establish a two-pronged approach involving OTC matrix and optimal cell combination for large-area bone regeneration *in vivo*.

Through this study, an effective MSC and EPC ratio was determined in a nude mouse subcutaneous pouch model. OTC matrix seeded with the bone and blood vessel forming cell combination potential for segmental bone defect repair was evaluated in a rabbit ulnar defect model. The objective of this study was to determine the best coculture composition of rabbit bone marrow-derived MSCs and PB-EPCs on optimally designed OTC matrices *in vivo* for vascularized and large-area bone regeneration.

Materials and Methods

Cell isolation

MSC isolation. Bone marrow-derived MSCs were isolated from New Zealand white rabbits.[35] Mononuclear cells were isolated via layering over a Percoll density gradient and centrifuging at 600 rpm for 20 min at room temperature. The mononuclear cell fraction was seeded and expanded in Dulbecco's modified Eagle's medium (DMEM; Invitrogen) supplemented with 10% fetal bovine serum (FBS) and 1% penicillin/streptomycin (P/S; Gibco) at 37°C and 5% CO_2. Passages 3–5 were used for experimentation.

PB-EPC isolation. Peripheral blood (50 mL) was collected via cardiac bleeding protocol (approved by the University of Connecticut Health Center Animal Care and Use Committee) from New Zealand white rabbits as previously reported.[35] Briefly, the mononuclear cell fraction was isolated by layering the peripheral blood over a Percoll density gradient and centrifuging at 600 rpm for 20 min at room temperature. The mononuclear cell fraction was resuspended in endothelial cell growth medium (EGM-2; composed of endothelial cell basal medium-2 [EBM-2], 10% FBS, 1% P/S, and EGM-2-SingleQuots growth factors and supplements; Lonza), immediately seeded on dishes coated with 1 μg/cm^2 of rabbit collagen type I (C5608; Sigma), and cultured at 37°C and 5% CO_2. Nonadherent cells were removed after 4–7 days by gentle washing with phosphate-buffered saline (PBS). Culture medium was changed every 3 days. Cells isolated 3–4 weeks postisolation (passages 5–8) were used for experiments. These PB-EPCs are referred as EPCs in the remainder of this article.

Scaffold fabrication

OTC matrices were fabricated using thermal sintering, followed by the porogen leaching method. Dr. Nukavarapu and his group have developed and effectively used this method to fabricate optimally porous and biomechanically compatible matrices (i.e., OTC matrices) for large-area bone regeneration[6,34,37] and gradient matrix systems for osteochondral tissue engineering.[38–40] Briefly, PLGA microspheres (diameter, 425–600 μm) and a porogen, NaCl crystals of diameter 200–300 μm, were mixed at a ratio of 4:1 by weight. The microsphere–salt mixture was packed into a steel mold and thermally sintered at 100°C for 1 h. NaCl particulates were leached out by soaking in water for 2 h. We fabricated and used disc-shaped matrices (10 mm diameter and 2 mm height) for *in vitro* studies and subcutaneous severe combined immunodeficiency (SCID) mice studies; we fabricated and used cylinder-shaped matrices (5 mm diameter and 15 mm height) for our critical-sized bone defect rabbit study model.

Evaluation of cell–scaffold construct performance in vitro

To assess the ability of the OTC matrices to support osteogenic and vasculogenic stem cell growth, MSCs and EPCs were seeded on the matrices and cultured for 2 days *in vitro*. Specifically, OTC matrices (20% NaCl:80% PLGA matrices) were seeded with a total of 250,000 cells per scaffold and cultured in a 1-to-1 mix of endothelial and osteogenic media for 2 days at 37°C and 5% CO_2. For immunofluorescence studies, we examined MSCs and EPCs cocultured at a ratio of 1:1 in a 1-to-1 mixture of osteogenic and angiogenic media. Before culture on matrices, MSCs were cultured in osteogenic media (DMEM, 10% FBS, 10 nM dexamethasone, 50 μg/mL ascorbic acid, and 5 mM β-glycerophosphate) on tissue culture plate (TCP) for 7 days.

MSC expression of osteogenic markers, RunX2 and collagen type I, and EPC expression of endothelial markers, CD31 and Von Willebrand factor (vWF), were analyzed by immunofluorescence. After 2 days *in vitro*, cell-seeded constructs were fixed in 10% formalin for 1 h at room temperature, rinsed with PBS, and permeabilized with 0.25% Triton X-100 for 10 min. Constructs were rinsed with PBS, blocked

in 10% normal goat serum for 1 h, and then incubated with the following primary antibodies for 1 h: anti-RunX2 antibody (ab76956, 1:50; Abcam), anticollagen I antibody (ab34710, 1:100; Abcam), anti-CD31 antibody (ab28364, 1:50; Abcam), anti-vWF antibody (ab6994, 1:1000; Abcam), and anti-β-tubulin (05-661, 1:200; Millipore). Samples were then washed and labeled with the corresponding secondary antibody: anti-mouse IgG secondary antibody–FITC (sc-2010; Santa Cruz) or anti-rabbit IgG secondary antibody–FITC (sc-2012; Santa Cruz) diluted 1:100 in 1% BSA/PBS for 40 min at room temperature. Finally, cell nuclei were counterstained using propidium iodide (81845; Sigma). Stained constructs were examined via confocal microscopy (20× magnification; Zeiss LSM ConfoCor2).

In vivo *performance evaluation of cell-seeded optimally porous matrices*

First, to evaluate the most effect ratio of MSCs and PB-EPCs seeded on our optimally porous matrices for the promotion of vascularization *in vivo*, we used an SCID mouse subcutaneous implant model. Second, we evaluated the performance with respect to vascularization and bone regeneration potential of our OTC matrices seeded with the most appropriate cell progenitor ratio and implanted in a rabbit ulnar bone defect model. The overall scheme of the study is presented in Figure 1.

SCID mouse subcutaneous implant model

Construct implantation. To evaluate the *in vivo* performance of various combinations of PB-EPC- and MSC-derived osteoblasts, we implanted the five construct conditions after 2 days *in vitro* to ensure proper cell adherence. We used only the cell-seeded constructs because our experiment aims to study the performance of cocultures, specifically on optimally prepared scaffolds. Constructs were prepared in the same manner as the *in vitro* constructs were prepared (250,000 cells total per scaffold). A 1-to-1 mixture of osteogenic and angiogenic media was used to culture grafts postseeding. We used acellular OTC matrices as negative controls. Five cell conditions seeded on matrices were examined: (1) MSC-derived osteoblasts, (2) EPCs, (3) coculture of four parts MSC-derived osteoblasts to one part EPC (4:1), (4) coculture of one part MSC-derived osteoblasts to one part EPC (1:1), and (5) coculture of one part MSC-derived osteoblasts to four parts EPC (1:4). Cell ratios were chosen to cover a wide range of possible ratios between the two cell populations based on our previous *in vitro* MSC–EPC coculture study.[35]

Male Fox Chase (CB17) SCID (Charles River Laboratories) mice were anesthetized with isoflurane in the induction chamber at a range of 3–5%. The animals were maintained on 2–4% isoflurane with the nose cone between placement of implants in separate subcutaneous dorsal pockets (two implants/animal and three animals/condition). The animals were postoperatively treated with the analgesic buprenorphine (0.05 mg/kg, subcutaneous). All animal experiments were approved by the University of Connecticut Health Center Animal Care and Use Committee (protocol 2009-593).

Histological staining and analysis. The implanted constructs were retrieved 8 weeks after implantation to analyze the blood vessel formation and bone formation. Samples were fixed overnight in 10% formalin and processed for paraffin sections. Histological staining was performed with Masson's trichrome stain (HT15; Sigma) on 5-μm-thick paraffin sections according to the manufacturer's protocol. Stained sections were analyzed under the light microscope Olympus BX50 with Olympus DP70 camera. For collagen quantification, we used the RBG plugin in ImageJ (National Institutes of Health), and specifically, collagen, which stains blue via Masson's trichrome staining, was quantified. While Masson's trichrome is often used to stain connective tissue, it is also used to stain collagen when studying *in vitro* and *in vivo* mineralization.[41,42]

Ten random images under 40× magnification were analyzed per sample (three samples/group; 30 total images per group) in ImageJ using the RBG Measure Plugin (http://rsb.info.nih.gov/ij/plugins/color-histogram.html) to measure the collagen stained blue with trichrome stain. Images were opened in ImageJ and converted to RBG Color (Image>Type>RBG Color), and then, the background was subtracted (Process>Subtract Background>Light Background); the RBG was measured on the selected region of interest. For vessel quantification, we analyzed and counted vascular structures in 10 random images taken under 20× magnification for each group.

Immunohistochemical analysis. To confirm vascularization and bone formation, we performed immunohistochemical analysis for endothelial markers CD31 and vWF

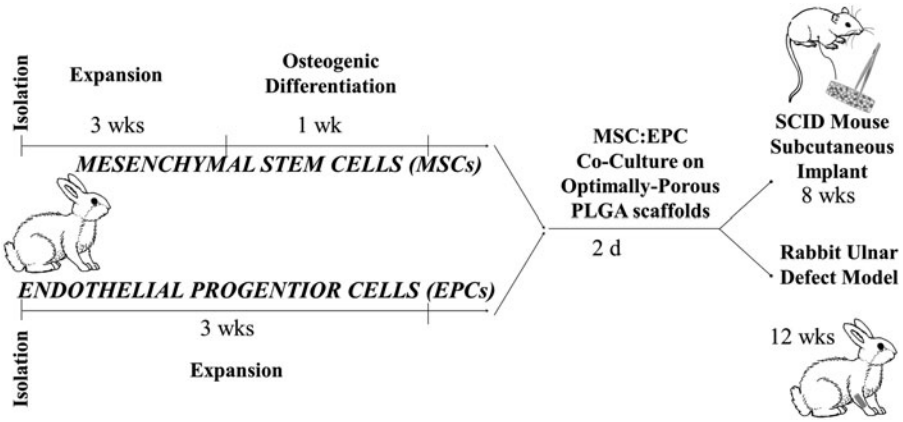

FIG. 1. Study plan for evaluating the vascular and bone regeneration potential of OTC matrices seeded with osteo- and vascular progenitor cells *in vivo*. OTC, oxygen tension controlled.

and bone markers RunX2 and collagen type I. We immunestained sections of the group containing the scaffold seeded with 1 part MSC-derived osteoblasts and 1 part EPC (1:1). We used paraffin-embedded mouse limbs (postnatal day 1) as a positive control. Briefly, rehydrated sections were exposed to heat-mediated antigen target retrieval (Target Retrieval Solution, Dako S1700) for 5 min at 98°C and then blocked in 10% normal goat serum in PBS for 1 h at room temperature.

Sections were incubated with the following primary antibodies overnight at 4°C: anti-RunX2 antibody (ab76956, 1:50; Abcam), anti-collagen I antibody (ab34710, 1:100; Abcam), anti-CD31 antibody (ab28364, 1:50; Abcam), anti-vWF antibody (ab6994, 1:1000; Abcam), and anti-β-tubulin (05-661, 1:200; Millipore). Samples were then washed and labeled with the corresponding secondary antibody: anti-mouse IgG secondary antibody–FITC (sc-2099; Santa Cruz) or anti-rabbit IgG secondary antibody–FITC (sc-53805; Santa Cruz) diluted 1:100 in 1% BSA/PBS for 40 min at room temperature. Finally, sections were mounted with propidium iodide/antifade solution (S7112; Millipore) and examined via confocal microscopy (20× magnification; Zeiss LSM ConfoCor2).

Rabbit critical-sized ulnar bone defect model

Construct implantation. Optimally porous matrices (20% NaCl:80% PLGA matrices; 15 mm height and 5 mm diameter) were seeded with a total of 500,000 cells/scaffold and cultured in a 1-to-1 mix of endothelial and osteogenic media for 2 days at 37°C and 5% CO_2. Before culture on matrices, MSCs were cultured in osteogenic media (DMEM, 10% FBS, 10 nM dexamethasone, 50 μg/mL ascorbic acid, and 5 mM β-glycerophosphate) on TCP for 7 days. Various cell conditions seeded on matrices were examined: (1) MSC-derived osteoblasts, (2) EPCs, (3) coculture of one part MSC-derived osteoblasts to one part EPC (1:1), and (4) acellular (i.e., scaffold alone). An empty defect control was not performed since a scaffold is necessary to physically stabilize the long-bone defect, and previous work has demonstrated acellular constructs as adequate controls.[43]

New Zealand white rabbits (4–5 kg weight) were anesthetized via an intramuscular injection of a mixture of ketamine (50 mg/kg), xylazine (6 mg/kg), and acepromazine (1 mg/kg). The right forelimb of the rabbit was shaved and prepped with Betadine and 70% ethanol. A longitudinal incision was made to expose the middiaphysis of the ulna. A segment of the ulna measuring 15 mm in length was removed using a bone saw. The matrices were implanted into the defect site, and the wound was closed by suturing muscles and skin in layers. After 12 weeks' implantation, animals were sacrificed, and ulnar bone was excised, fixed in 10% formalin for 24 h, and then transferred to 70% ethanol until further analysis.[43]

Micro-CT analysis. Micro-CT provides an efficient method to measure the distribution and density of mineralized tissue throughout the scaffold. Limbs harvested at week 12 were imaged using cone beam microfocus X-ray computed tomography to render three-dimensional models for direct quantitation of sample bone density and volume and to provide a three-dimensional reconstruction of the defect (μCT40; Scanco Medical AG). Segmentation of bone and scaffold provided direct volumetric quantification of bone formation into the depths of the scaffold, as well as the analysis of the structural integrity of new bone and biodegradable scaffold. Mass was calibrated to a stepped hydroxyapatite phantom (item no. KP-03-03; Scanco) expressed as milligrams of hydroxyapatite per cubic centimeter.

Serial tomographic images were acquired at 55 kV and 145 μA with a 300-ms integration time. A set length of 11 mm was analyzed within the defect. Measurements include volumetric basis, but accurate measures are based on mass, which captures all mineral including what is not taken into account in volume measurements of repairing bone with low-density regions. Mass is calibrated to a stepped hydroxyapatite phantom expressed as milligrams of hydroxyapatite per cubic centimeter. Since the bone remodeling is significant, such that formation/resorption/remodeling is not distinguishable and includes regions of high and low density, to measure all formation, the total mass of all bone (radius, callus, everything) was measured within the set length. We also measured and subtracted off the mass of the radius in the intact limb within the matching region of each experimental limb.

Histological staining and analysis. Limbs were embedded in methyl methacrylate using a slow methyl methacrylate (sMMA) processing, infiltration, and embedding techniques, as described by Kecena *et al.*, then sectioned at 7 μm thickness with a Reichert–Jung polycut E microtome and a tungsten carbide D profile knife (Dornt Hart), and mounted onto glass slides. These sections were then be stained with hematoxylin and eosin to evaluate cellular events, von Kossa to evaluate all the mineralized tissues at the site, and Goldner's trichrome to evaluate the osteoid or new unmineralized bone being deposited at bone forming sites.[43,44]

Statistical analysis

For vascular and bone quantification analysis (i.e., histology and micro-CT), a one-way analysis of variance (ANOVA) was performed to compare data. Error is reported in figures as the standard deviation (SD), and significance was determined using $p < 0.05$.

Results

Cell-seeded constructs in vitro *evaluation*

Cell-seeded OTC matrices were evaluated after 2 days in culture (i.e., preimplantation stage) (Fig. 2). Both MSC-derived osteoblasts and EPCs retained their differentiations in coculture (1:1). As seen in Figure 2, EPCs retained the endothelial cell phenotype in coculture, as demonstrated by positive immune staining of CD31 and vWF. Furthermore, MSC-derived osteoblasts maintained differentiation in coculture, as indicated by positive immune staining of Col I and RunX2 (green). Cell nuclei staining (red) confirms that positive staining for MSC and EPC markers is cell derived. Therefore, OTC matrices coseeded with MSC and EPC demonstrate coexistence of both bone and vessel forming cells before *in vivo* implantation. Although the study presented a coculture of MSCs and EPCs in a 1:1 ratio as a representative group, we observed that this matrix system is capable of supporting any ratio of MSC and EPC cocultures.[34]

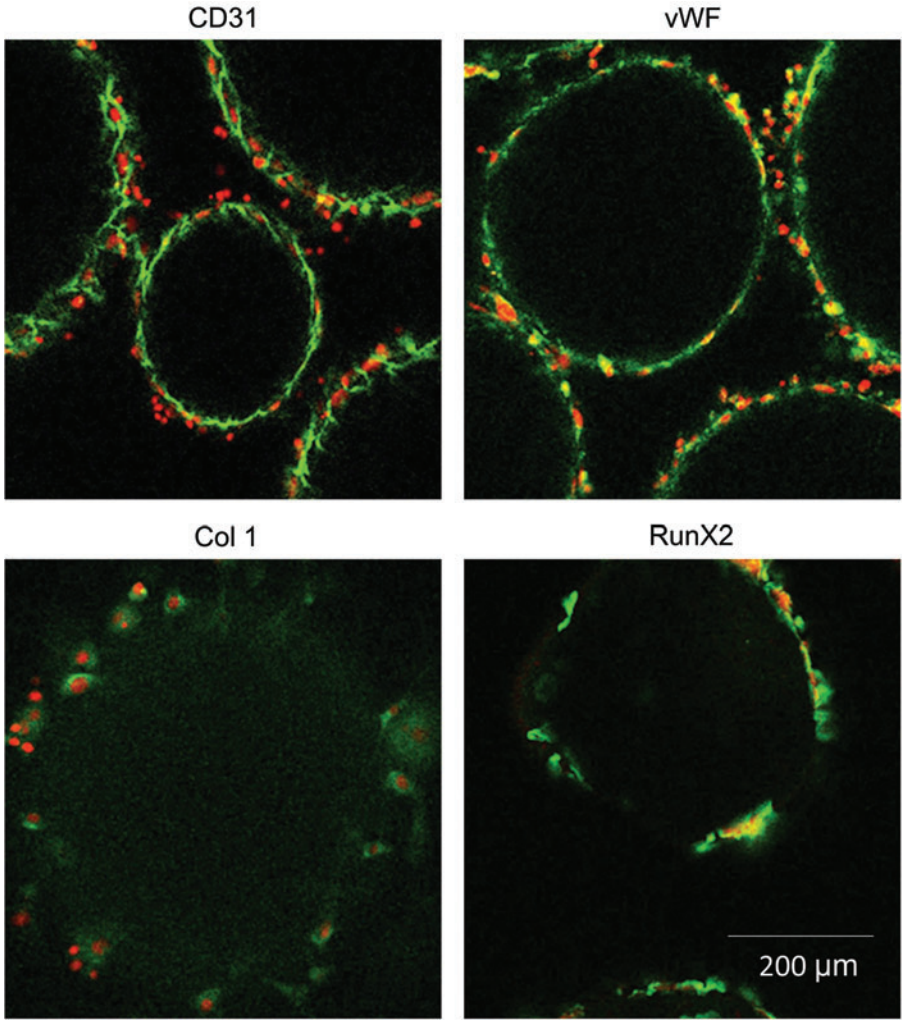

FIG. 2. Immunofluorescence staining of endothelial cell markers CD31 and vWF and osteogenic markers Col I and RunX2 on coculture of MSC:EPC (1:1) constructs preimplantation. EPC, endothelial progenitor cell; MSC, mesenchymal stem cell; vWF, Von Willebrand factor. Color images available online at www.liebertpub.com/tea

Cell-seeded constructs in vivo *evaluation*

SCID mouse subcutaneous model. Two-day precultured *in vitro* matrices were implanted for 8 weeks subcutaneously in SCID mice, at which point, they were harvested for histological analysis (as per the protocol depicted in Fig. 1). Matrices of various MSC-derived osteoblast:EPC (OB:EPC) coculture ratios were evaluated, and matrices of each cell type seeded alone served as controls, as well as acellular constructs. Matrices were paraffin embedded, sectioned, and processed for immunostaining and Masson's trichrome staining (Fig. 3). The staining showed blue color corresponding to collagen or bone formation and red color associated with vascularization in all the matrices, except the acellular control. However, adipose tissue formation is prominently seen with the acellular matrices.

We analyzed and quantified collagen formation histologically (Fig. 3). Specifically, we performed a colorimetric quantification analysis (RBG plugin, ImageJ, NIH) on Masson's trichrome-stained paraffin-embedded sections of the constructs. Since the Masson's trichrome staining procedure results in blue-stained collagen and bone, we used the RBG Measure Plugin tool in ImageJ to measure the blue staining collagen/bone.[41,42] In this manner, we observed significant collagen formation in constructs cultured with MSC-derived osteoblasts, as well as those cocultured with MSC-derived osteoblasts and EPCs at all examined ratios (i.e., 4:1, 1:1, and 1:4) compared to acellular constructs after 8 weeks *in vivo*. However, in comparison to collagen formation in constructs seeded with MSC-derived osteoblasts, only those seeded with cocultured MSC-derived osteoblasts and EPCs at ratios of 4:1 and 1:1 demonstrated significant collagen formation. It is important to note that all the constructs showed some level of lipoid tissue, which is removed during embedding, resulting in alveolar structure formation, as marked in Figure 3. Acellular control showed the highest levels of lipoid tissue, while the remaining groups presented traces of it.

Vascular formation analysis throughout the constructs was also performed on the trichrome-stained sections. Implantation of EPCs significantly enhanced vascularization throughout the constructs. As seen in Figure 3, constructs seeded with EPCs demonstrated significantly more vascularization than those that were initially implanted without cells. However, constructs coseeded with MSC-derived osteoblasts and EPCs at a ratio of 1:1 (1 OB:1 EPC) demonstrated the highest level of vascularization. Implantation of constructs coseeded with MSC-derived osteoblasts and EPCs at a ratio of 1:4 did result in significant vascularization compared to acellular constructs, however, lower than that of EPC-seeded and 1:1 (1 OB:1 EPC)-seeded constructs. Qualitative assessment of vascular,

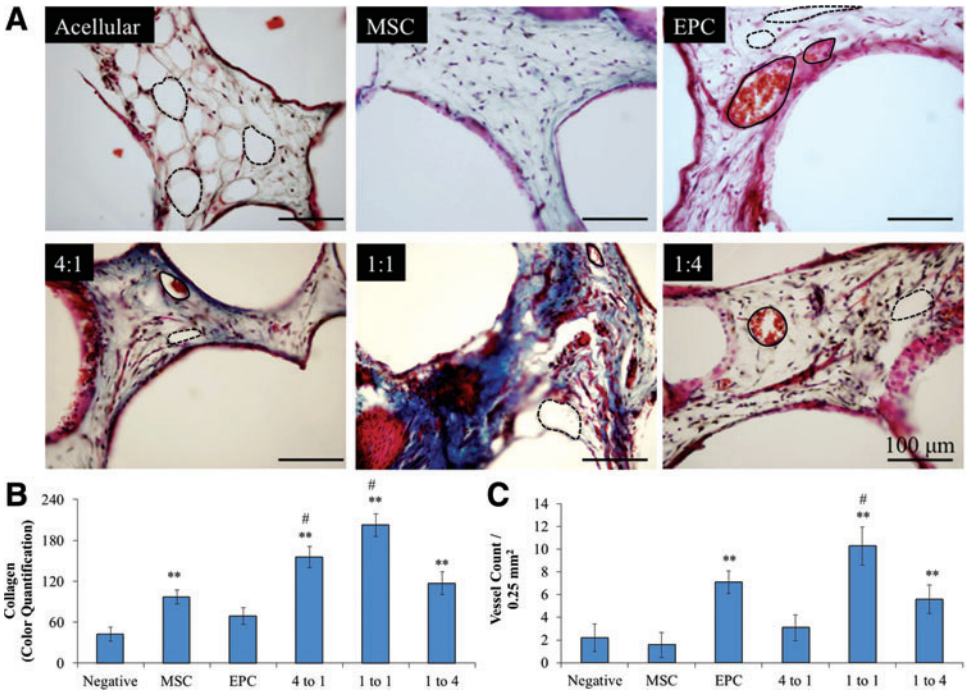

FIG. 3. **(A)** Masson's trichrome staining on acellular, MSC-seeded, EPC-seeded, 4 MSC:1 EPC-seeded, 1 MSC:1 EPC-seeded, and 1 MSC:4 EPC-seeded constructs 8 weeks postimplantation. Alveolar structures indicated by *dashed lines*, and vascular structures indicated with *solid lines*. **(B)** Quantification of collagen staining (**significance compared to negative, $p < 0.05$; #significance compared to EPC, $p < 0.05$). **(C)** Quantification of *in vivo* vascularization (**significance compared to negative, $p < 0.05$; #significance compared to MSC, $p < 0.05$). Color images available online at www.liebertpub.com/tea

collagen, and adipose tissue formation is shown in Figure 4. Thus, 1 OB:1 EPC construct showed the highest level of vascularization and collagen formation. Vessel formation was confirmed via CD31 and vWF immunostaining, and bone formation was confirmed via collagen type 1 (Col I) and RunX2 immunostaining (Fig. 4). For this study, we used 1-day-old mouse embryo limbs as a positive control.

Rabbit ulnar critical-sized bone defect model. A 15-mm bone defect was created in the ulnar bone of New Zealand white rabbits (4–5 kg), and an OTC matrix (cylinder of 5 mm diameter and 15 mm height) was inserted into the bone defect. The construct was previously seeded with a total of 250,000 cells, in 1-to-1 ratio of MSCs and EPCs (125,000 MSCs and 125,000 EPCs), or no cells (i.e., acellular construct to serve as a negative control) and cultured for 2 days in a 1-to-1 mix of osteogenic and endothelial growth media (as per the protocol in Fig. 1). We examined six rabbits for each group (i.e., four groups: acellular, MSC, EPC, and 1:1 MSC:EPC).

Rabbits were monitored closely for their recovery and performance. Several days to 1 week postoperation, all rabbits were sitting up, walking, eating, drinking, and performing as expected for postoperation. Rabbits were fully functioning in their movements (i.e., walking, running, and jumping) and applying weight on their forearms (including their arm that was operated on) at 6 and 12 weeks postoperation. After 12 weeks, all rabbits were sacrificed for analysis and evaluation of bone and vascular regeneration at the bone defect.

Micro-CT analysis was used to evaluate bone regeneration at the defect site. Significant remodeling and callus formation were observed in most bone specimens, such that formation, resorption, and/or remodeling are not distinguishable, and

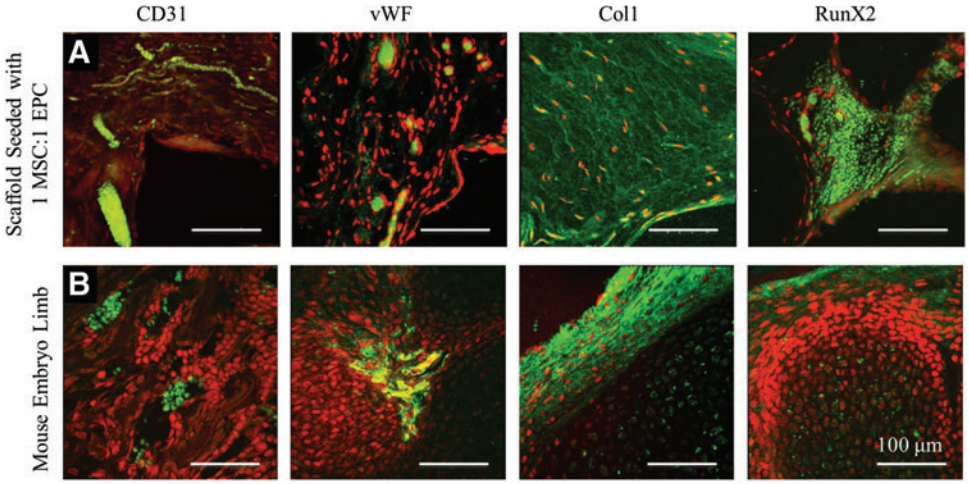

FIG. 4. Immunofluorescence staining of endothelial markers CD31 and vWF and osteogenic markers RunX2 and collagen type I on **(A)** construct preseeded with MSC:EPC and **(B)** mouse limb postnatal day 1 (positive control). Color images available online at www.liebertpub.com/tea

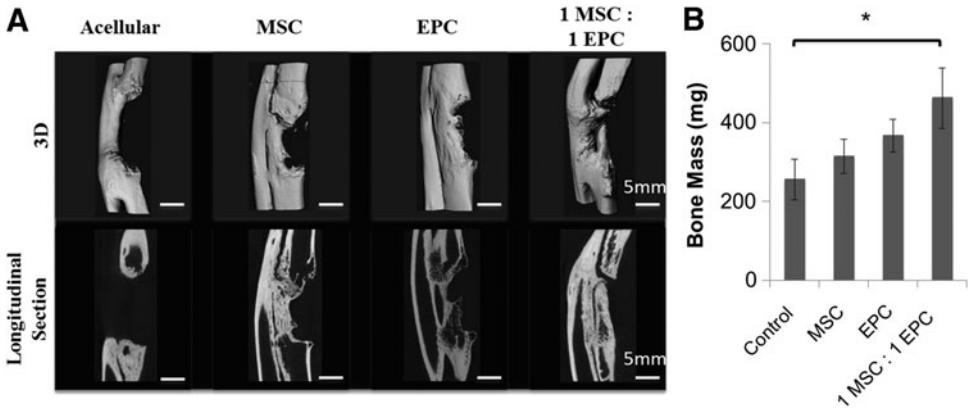

FIG. 5. Micro-CT analysis of ulnar bone defect 12 weeks postimplantation. **(A)** Three-dimensional reconstructed images and longitudinal section images are shown for each group (i.e., acellular, MSC-seeded, EPC-seeded, and a 1:1 ratio of MSC:EPC-seeded constructs). Scale bar = 5 mm. **(B)** Bone mass in the ulnar bone defect. $*p < 0.05$.

include regions of high and low density. Therefore, to measure all bone formation, the total mass of all bone (i.e., ulnar, radius, and callus) within the set length was measured. In addition, the mass of the radius in the intact limb was also measured. To quantify the mass and bone volume within the ulnar defect, the mass of the intact radius was subtracted off the mass of the experimental limb. Bone volume estimation is often used to quantify the regenerated bone or new mineralization.[45] Since the remodeling/integrated radius in the present case cannot be distinguished from formation in the segmental defect, the radius was included, and then, a single scalar reference magnitude of bone mass for an 11-mm segment of control radius was subtracted from the measurement of mass for each animal to provide a proper estimate of formation mass.

Limited bone regeneration was observed in the acellular group, which confirmed this model as a critical-sized bone defect (Fig. 5). The MSC and EPC groups displayed higher levels of bone regeneration than the acellular group (Fig. 5B). However, the rabbit group that received constructs seeded with 1-to-1 ratio of MSCs and EPCs displayed significantly higher levels of bone regeneration than that of the acellular group. As seen by the longitudinal sections in Figure 5A, all the groups other than the acellular group displayed partial bone bridging throughout the thickness of the defect. However, the OTC scaffold seeded with one-to-one MSC to EPCs demonstrated the highest amount of regenerated bone mass.

Histological analysis of von Kossa-stained sections confirmed the findings from micro-CT analysis (Fig. 6 A, B). The acellular group displayed a lack of mineralized tissue within the defect, whereas the cell-seeded groups with MSCs and EPCs showed increased bone mineralization located at the bony edges of the bone defect. Moreover, the 1:1 MSC:EPC-seeded construct group displayed the highest amount of the bone mineralization not just localized to the bony edge of the defect, but also, there are signs of attempted bony bridging. Quantitative analysis of the von Kossa-stained sections demonstrated a significant increase in mineralized bone area in the MSC- and EPC-seeded groups compared to acellular constructs; however, their levels are not significantly different from each other. The coculture 1:1 MSC:EPC-seeded group displayed the most significant increase in mineralized bone area compared to the acellular group (Fig. 6B).

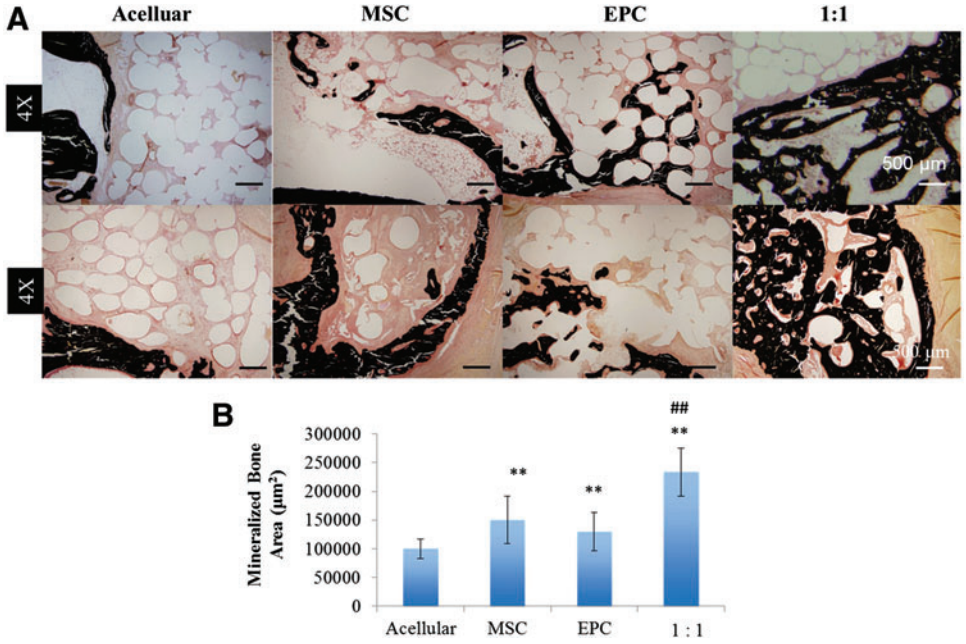

FIG. 6. **(A)** Representative histological images of von Kossa-stained longitudinal (*top*) and cross-sectional (*bottom*) samples under 4× magnification. **(B)** Quantification of mineralized bone area formed within the rabbit ulnar defect. Three regions on von Kossa-stained sections were analyzed from three samples in each group under low magnification with a thresholding analysis tool from ImageJ software. $**p < 0.05$, $^{\#\#}p < 0.001$. Color images available online at www.liebertpub.com/tea

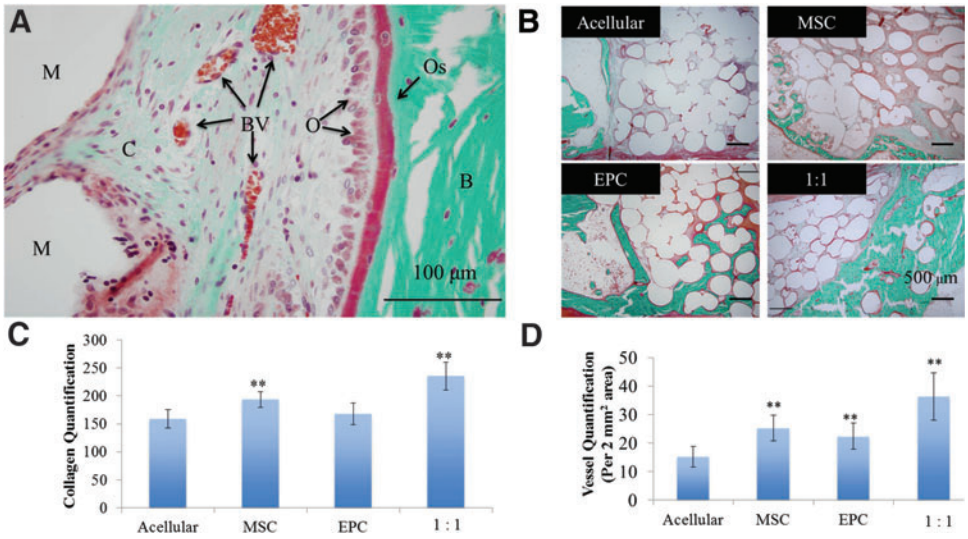

FIG. 7. **(A)** Labeled Goldner's trichrome-stained section imaged under 40× (scale bar = 100 μm). **(B)** Representative histological images of Goldner's trichrome-stained longitudinal sections under 10× magnification. **(C)** Quantification of vessels within the rabbit ulnar defect. Vessels were counted in five regions on trichrome-stained sections under 10× magnification for three samples in each group. **(D)** Quantification of collagen formation within the rabbit ulnar defect. Ten regions on trichrome-stained sections were analyzed for the intensity of collagen (*green*) from three samples in each group under 20× magnification with a color (RBG) histogram analysis tool from ImageJ software (arbitrary scale of 0–255, with 255 representing the highest *green* intensity). $^{**}p < 0.05$. M, microsphere scaffold; C, unmineralized collagen; BV, blood vessel; O, osteoblast; Os, osteoid; B, mineralized bone. Color images available online at www.liebertpub.com/tea

Similar trends were observed with unmineralized bone formation with Goldner's trichrome staining (Figs. 7B, 7C). Green staining represents collagen deposition, with the increased intensity being mineralized collagen formation. Red staining represents fibrous tissue formation. The acellular group showed limited collagen deposition and increased levels of adipose tissue deposition. The MSC- and EPC-seeded groups displayed mineralized bone formation within the defect, as well as some unmineralized bone formation. However, the 1:1 MSC:EPC-seeded group displayed the highest levels of mineralized and unmineralized bone formation within the bone defect (Fig. 6B and Fig. 7C). In addition, the 1:1 MSC:EPC-seeded group displayed the highest and most significant levels of vascularization, with the MSC- and EPC-seeded groups also displaying increased vascularization compared to the acellular group (Fig. 7D).

Discussion

Bone tissue engineering research has revealed tremendous potential for the treatment of bone defects.[1–3] The bone tissue engineering paradigm classically involves the combination of one or more of the following components: a mechanically compatible scaffold, effective cell populations, and/or growth factors. However, central necrosis or lack of bone tissue formation due to the lack of, or insufficient, vascularization of bone constructs is a well-recognized obstacle to the success of complete bone regeneration and host integration in bone tissue engineering.[46] This is mainly due to the lack of matrix systems that support seeded cells before the matrix vascularization. Our group developed OTC matrices that support bone and vessel forming cells throughout the pore structure.[6,34,36] We chose such a matrix system in this study to demonstrate large-area bone regeneration *in vivo*.

In the present study, we aimed to identify effective cell populations for enhanced bone formation and vascularization. We examined EPCs as an effective endothelial population since they have been previously proven to promote vascularization and, in turn, promote successful bone formation at the graft site.[47] Additionally, EPCs display high angiogenic, proliferative, and survival potential *in situ*.[21,48,49] Furthermore, PB-EPCs cultured simultaneously with MSCs displayed significantly enhanced expression levels of key osteogenic and vascular markers, including bone morphogenetic protein 2, and VEGF.[12,28,35,50,51] Therefore, we identified the highly angiogenic PB-EPCs as an ideal autologous cell population since their isolation does not risk donor site morbidity, and importantly, they effectively result in enhanced vascularization as well as successful engineered bone tissue regeneration.

We proposed a two-pronged approach for vascularized bone tissue engineering, the two prongs being an optimal scaffold and effective progenitor cells. Our work in optimal scaffold design resulted in the development of OTC matrices that support cell survival throughout the scaffold pore volume.[36] In this study, OTC matrices are characterized, specifically by seeding with bone and blood vessel forming cells together. Matrices seeded with MSCs and EPCs demonstrated not only their survival and growth but also their functionality through the expression of osteogenic and vasculogenic markers, respectively, deep inside the scaffold.

With the identification of an optimal matrix system, we set forward to investigate the most effective cell ratio of MSC-derived osteoblasts and EPCs for *in vitro* prevascularization, as well as subsequent neovascularization and bone formation *in vivo*. MSC to EPC ratios of 4:1, 1:1, and 1:4 were chosen to adequately cover a wide range of possible ratios to study MSCs and EPCs in coculture in the

OTC matrices. As per our previous study, these ratios showed synergy in terms of osteogenic as well as angiogenic gene expressions.[6] Our previous data demonstrated that MSC-seeded constructs were positive for osteogenic markers, and EPC-seeded constructs were positive for vascular endothelial markers.[36] This study was intended to see whether MSC and EPC in coculture demonstrate the same functionality deep inside the matrix. Immunofluorescence staining of the OTC matrices cocultured with MSCs and EPCs confirms the maintenance of the endothelial cell markers (i.e., CD31 and vWF) by EPCs and osteogenic cell markers (i.e., collagen type I and RunX2) by MSCs postseeding onto the three-dimensional matrix (Fig. 2).

Constructs seeded with MSCs and EPCs at a ratio of 1:1 demonstrated not only the highest level of vascularization throughout the implant construct but also collagen formation after 8 weeks *in vivo* (Fig. 3). Although matrices seeded with EPCs alone, as well as in coculture with MSC-derived osteoblasts (ratio of 1:4), also demonstrated significant vascular formation throughout the matrix compared to acellular matrices, it was significantly less than that of matrices seeded with the cells at a 1:1 ratio. In addition, significant collagen formation was observed throughout all the matrices that were seeded with both cell types at all ratios (1:4, 1:1, and 4:1), as well as those seeded with MSC-derived osteoblasts. However, once again, matrices seeded with MSC-derived osteoblasts and EPCs at a ratio of 1:1 resulted in the highest levels of collagen formation. Vascular and bone formation *in vivo* was confirmed through immunostaining of endothelial markers CD31 and vWF, as well as osteogenic markers collagen type I and RunX2. Bone regeneration involves vascularization and mineralization events. Results here suggest increased bone formation when used bone and blood vessel forming cells in equal amounts, 1:1 ratio. Although MSC and EPC cocultures were studied for bone regeneration *in vitro* and *in vivo*, we believe it is the first study of its kind where the optimal MSC:EPC cocultures in an OTC matrix is established in a subcutaneous model.

Acellular samples showed the highest levels of adipose tissue formation upon subcutaneous implantation, likely due to the lack of progenitor cells promoting osteogenesis and vasculogenesis. In regard to the observed adipose tissue, we speculate the absence of a strong angio-/osteoinductive environment in the case of the MSC, EPC, and their combinations. However, it is established from this study that MSC and EPC synergy along with the osteogenic and vasculogenic media preculture treatment promotes osteogenesis and vasculogenesis *in vivo*. Immunohistochemical analysis of MSC to EPC one-to-one group was to directly establish osteogenic (through col I and RunX2 staining) as well as vasculogenic (through CD31 and vWF staining) ability of these samples upon subcutaneous implantation. Immunofluorescence imaging, presented in Figure 4, demonstrates the functionality of the newly formed blood vessels as they show a collection of RBCs in the cross section of the vascular lumens without extravasation.

With the collagen and vessel count quantification data, we selected the ratio of 1:1 MSC:EPC as the most effective progenitor cell ratio and pursued a load-bearing bone defect model. We evaluated the performance of four different groups: acellular matrices, MSC-seeded matrices, EPC-seeded matrices, and a coculture of MSCs and EPCs at a ratio of 1:1. Scaffold mineralization associated with the cell-seeded groups suggests loaded-cell-induced bone formation, especially when no visual mineralization is seen with the scaffold-alone group. The proximal and distal ulna of the 1 MSC:1 EPC group in Figure 5 appears to be capped with bone. We believe that the regenerated tissue is not completely mineralized; therefore, it is partially bridged and appears not to be communicating. Partial bridging/presence of unmineralized tissue could be attributed to two factors: (1) lack of a strong osteo-/vasculogenic environment and (2) implant analysis at early time points, such as 12 weeks. However, the coculture group 1:1 outperformed and displayed the most significant increase in bone formation and vascularization with the bone defect as confirmed by micro-CT and histological analysis.

Collagen matrix deposition and mineralization are observed throughout the scaffold pore structure for the MSC and EPC coimplantation group. However, the MSC-alone group showed collagen deposition and mineralization limited to the scaffold surface despite their culture on OTC matrices. The results suggest that MSC and EPC cocultures on OTC matrices results in vascularized bone formation. The EPC-seeded matrix group showed collagen deposition and mineralization better than the MSC group. This is because of the fact that EPCs are known to induce early vascularization and thus can support osteogenesis of the graft invading MSC population.[10–12,52] Such a scenario is not possible with the matrix+MSC and the matrix-alone groups; therefore, it is expected to see the majority of the matrix invading cell population turning into fibroblasts or adipose cells. Our results show that the least amount of adipose and fibrous tissue formation occurred with the coculture and EPC groups compared to the acellular group and MSC-seeded group.

Using MSC and EPC synergy for vascularized bone regeneration has been a new paradigm in bone tissue engineering. Fedorovich *et al.* have discussed the role of EPCs in MSC mineralization.[50] Our group established PB-EPCs as superior cell population over the bone marrow-derived EPCs for synergy with MSCs. We have studied this extensively *in vitro* to find that the optimal ratio of bone marrow-derived MSCs and PB-EPCs for vascularized bone regeneration was a ratio of 1:1.[35] Vascularized bone formation *in vitro* with PB-EPCs and MSCs has been demonstrated by Fu *et al.*[24] Seebach *et al.* demonstrated enhanced neovascularization in bone regeneration using human bone marrow-derived MSCs and EPCs from buffy coat seeded onto b-TCP granules for large bone defects in rats.[12] Our current work establishes an optimum coculture ratio of bone marrow-derived MSCs and PB-EPCs, as well as confirms their synergy in an optimum OTC matrix for enhanced osteogenesis and vascularization in a subcutaneous model and large-area bone regeneration in a functional defect model. Overall, this study is establishing a two-pronged approach (involving OTC matrices and effective progenitors) for vascularized bone tissue engineering. However, long-term studies comparing the performance with an osteoinductive factor group are necessary to further establish the clinical potential of this new approach for bone defect repair.

Conclusions

Through this study, we have identified the most effective cell ratio of MSC-derived osteoblasts to EPCs, two easily accessible autologous cell sources. Furthermore, we proposed

and implemented a two-pronged approach, using OTC matrices and optimal ratio of effective progenitor cells, for the enhanced repair and regeneration of a critically sized load-bearing bone defect in rabbits. The synergy between MSCs and EPCs is used to develop a nongrowth factor approach for vascularized bone formation. OTC matrix in conjunction with the effective progenitors led to large-area and vascularized bone regeneration, which is critical to heal large and segmental bone defects via bone tissue engineering.

Acknowledgments

Dr. Nukavarapu acknowledges funding from the AO Foundation (startup grant: S-13-122N). The authors acknowledge support from the Musculoskeletal Transplant Foundation (MTF), NSF (EFRI# 1332329), NIH (BUILD# 8RL5GM118969), and Connecticut Institute for Clinical and Translational Science (CICATS) at the University of Connecticut. Ms. A.R.A. thank NIH F30DE022477 award for financial support. The authors thank Dr. Adams and Vilmaris Diaz-Doran for their help with the micro-CT work.

Disclosure Statement

No competing financial interests exist.

References

1. Amini, A.R., Laurencin, C.T., and Nukavarapu, S.P. Bone tissue engineering: recent advances and challenges. Crit Rev Biomed Eng **40,** 363, 2012.
2. Nukavarapu, S.P., Freeman, J.W., and Laurencin, C.T. Regenerative Engineering of Musculoskeletal Tissues and Interfaces. New York: Woodhead Publishing, 2015.
3. Petite, H., Viateau, V., Bensaïd, W., Meunier, A., Pollak, C., Bourguignon, M., et al. Tissue-engineered bone regeneration. Nat Biotechnol **18,** 959, 2000.
4. Dimitriou, R., Jones, E., Mcgonagle, D., and Giannoudis, P.V. Bone regeneration: current concepts and future directions. BMC Med **9,** 2011; DOI: 10.1186/1741-7015-9-66.
5. Bose, S., Roy, M., and Bandyopadhyay, A. Recent advances in bone tissue engineering scaffolds. Trends Biotechnol **30,** 546, 2012.
6. Amini, A.R., Adams, D.J., Laurencin, C.T., and Nukavarapu, S.P. Optimally porous and biomechanically compatible scaffolds for large-area bone regeneration. Tissue Eng Part A **18,** 1376, 2012.
7. Karageorgiou, V., and Kaplan, D. Porosity of 3D biomaterial scaffolds and osteogenesis. Biomaterials **26,** 5474, 2005.
8. Rezwan, K., Chen, Q.Z., Blaker, J.J., and Roberto, A. Biodegradable and bioactive porous polymer/inorganic composite scaffolds for bone tissue engineering. Biomaterials **27,** 3413, 2006.
9. Tsigkou, O., Pomerantseva, I., Spencer, J.A., Redondo, P.A., Hart, A.R., Sundback, C.A., et al. Engineered vascularized bone grafts. Proc Natl Acad Sci USA **107,** 3311, 2010.
10. Usami, K., Mizuno, H., Okada, K., Narita, Y., Aoki, M., Kondo, T., et al. Composite implantation of mesenchymal stem cells with endothelial progenitor cells enhances tissue-engineered bone formation. J Biomed Mater Res A **90,** 730, 2009.
11. Henrich, D., Seebach, C., Kaehling, C., Scherzed, A., Wilhelm, K., Tewksbury, R., et al. Simultaneous cultivation of human endothelial-like differentiated precursor cells and human marrow stromal cells on beta-tricalcium phosphate. Tissue Eng Part C Methods **15,** 551, 2009.
12. Seebach, C., Henrich, D., Kähling, C., Wilhelm, K., Tami, A.E., Alini, M., et al. Endothelial progenitor cells and mesenchymal stem cells seeded onto beta-TCP granules enhance early vascularization and bone healing in a critical-sized bone defect in rats. Tissue Eng Part A **16,** 1961, 2010.
13. Zhou, J., Lin, H., Fang, T., Li, X., Dai, W., Uemura, T., et al. The repair of large segmental bone defects in the rabbit with vascularized tissue engineered bone. Biomaterials **31,** 1171, 2010.
14. Mauney, J.R., Volloch, V., and Kaplan, D.L. Role of adult mesenchymal stem cells in bone tissue engineering applications: current status and future prospects. Tissue Eng **11,** 787, 2005.
15. Kagami, H., Agata, H., and Tojo, A. Bone marrow stromal cells (bone marrow-derived multipotent mesenchymal stromal cells) for bone tissue engineering: basic science to clinical translation. Int J Biochem Cell Biol **43,** 286, 2011.
16. Nukavarapu, S., Amini, A.R., and Wallace, J.S. Short-term and long-term effects of orthopedic biogegradable implants. J Long Term Eff Med Implants **21,** 93, 2011.
17. Griffin, M., Iqbal, S.A., and Bayat, A. Exploring the application of mesenchymal stem cells in bone repair and regeneration. J Bone Joint Surg Br **93,** 427, 2011.
18. Volkmer, E., Drosse, I., Otto, S., Stangelmayer, A., Stengele, M., Kallukalam, B.C., et al. Hypoxia in static and dynamic 3D culture systems for tissue engineering of bone. Tissue Eng Part A **14,** 1331, 2008.
19. Logeart-Avramoglou, D., Anagnostou, F., Bizios, R., and Petite, H. Engineering bone: challenges and obstacles. J Cell Mol Med **9,** 72, 2005.
20. Eiselt, P., Kim, B.S., Chacko, B., Isenberg, B., Peters, M.C., Greene, K.G., et al. Development of technologies aiding large-tissue engineering. Biotechnol Prog **14,** 134, 1998.
21. Asahara, T., and Kawamoto, A. Endothelial progenitor cells for postnatal vasculogenesis. Am J Physiol Cell Physiol **287,** C572, 2004.
22. Finkenzeller, G., Torio-Padron, N., Momeni, A., Mehlhorn, A.T., and Stark, G.B. In vitro angiogenesis properties of endothelial progenitor cells: a promising tool for vascularization of ex vivo engineered tissues. Tissue Eng **13,** 1413, 2007.
23. Kaully, T., Kaufman-Francis, K., Lesman, A., and Levenberg, S. Vascularization—the conduit to viable engineered tissues. Tissue Eng Part B Rev **15,** 159, 2009.
24. Fu, W.L., Xiang, Z., Huang, F.G., Gu, Z.P., Yu, X.X., Cen, S.Q., Zhong, G., Duan, X., Duan, X., and Liu, M. Coculture of peripheral blood-derived mesenchymal stem cells and endothelial progenitor cells. Tissue Eng Part A **21,** 948, 2015.
25. Yu, H., Vandevord, P.J., Mao, L., Matthew, H.W., Wooley, P.H., and Yang, S. Biomaterials improved tissue-engineered bone regeneration by endothelial cell mediated vascularization. Biomaterials **30,** 508, 2009.
26. Rouwkema, J., Westerweel, P.E., Boer, J., et al. The use of endothelial progenitor cells for prevascularized bone tissue engineering. Tissue Eng Part A **15,** 2009.
27. Matsumoto, T., Kawamoto, A., Kuroda, R., Ishikawa, M., Mifune, Y., Iwasaki, H., et al. Therapeutic potential of vasculogenesis and osteogenesis promoted by peripheral blood CD34-positive cells for functional bone healing. Am J Pathol **169,** 1440, 2006.
28. Aguirre, A., Planell, J.A., and Engel, E. Dynamics of bone marrow-derived endothelial progenitor cell/mesenchymal

stem cell interaction in co-culture and its implications in angiogenesis. Biochem Biophys Res Commun **400,** 284, 2010.
29. Ern, C., Krump-Konvalinkova, V., Docheva, D., Schindler, S., Rossmann, O., Böcker, W., et al. Interactions of human endothelial and multipotent mesenchymal stem cells in cocultures. Open Biomed Eng J **4,** 190, 2010.
30. Mayer, H., Bertram, H., Lindenmaier, W., Korff, T., Weber, H., and Weich, H. Vascular endothelial growth factor (VEGF-A) expression in human mesenchymal stem cells: autocrine and paracrine role on osteoblastic and endothelial differentiation. J Cell Biochem **95,** 827, 2005.
31. Beckermann, B.M., Kallifatidis, G., Groth, A., Frommhold, D., Apel, A., Mattern, J., et al. VEGF expression by mesenchymal stem cells contributes to angiogenesis in pancreatic carcinoma. Br J Cancer **99,** 622, 2008.
32. Kaigler, D., Krebsbach, P.H., Polverini, P.J., and Mooney, D.J. Role of vascular endothelial growth factor in bone marrow stromal cell modulation of endothelial cells. Tissue Eng **9,** 95, 2003.
33. Smadja, D.M., Bièche, I., Silvestre, J.S., Germain, S., Cornet, A., Laurendeau, I., et al. Bone morphogenetic proteins 2 and 4 are selectively expressed by late outgrowth endothelial progenitor cells and promote neoangiogenesis. Arterioscler Thromb Vasc Biol **28,** 2137, 2008.
34. Nukavarapu, S.P., and Amini, A.R. Optimal scaffold design and effective progenitor cell identification for the regeneration of vascularized bone. Conf Proc IEEE Eng Med Biol Soc **2011,** 2464, 2011.
35. Amini, A.R., Laurencin, C.T., and Nukavarapu, S.P. Differential analysis of peripheral blood- and bone marrow-derived endothelial progenitor cells for enhanced vascularization in bone tissue engineering. J Orthop Res **30,** 1507, 2012.
36. Amini, A.R., and Nukavarapu, S.P. Oxygen-tension controlled matrices for enhanced osteogenic cell survival and performance. Ann Biomed Eng **42,** 1261, 2014.
37. Igwe, J.C., Mikael, P.E., and Nukavarapu, S.P. Design, fabrication and in vitro evaluation of a novel polymer-hydrogel hybrid scaffold for bone tissue engineering. J Tissue Eng Regen Med **8,** 131, 2014.
38. Majumdar, S., Pothirajan, P., Dorcemus, D., Nukavarpu, S., and Kotecha, M. High field sodium MRI assessment of stem cell chondrogenesis in a tissue-engineered matrix. Ann Biomed Eng 2015 [Epub ahead of print]; DOI: 10.1007/s10439-016-1548-z.
39. Dorcemus, D.L., and Nukavarapu, S.P. Novel and unique matrix design for osteochondral tissue engineering. MRS Proc **1621,** 17, 2014.
40. Nukavarapu, S.P., Laurencin, C.T., Amini, A.R., and Dorcemus, D.L. Gradient porous scaffolds. U.S. Patent US20140178455 A1, December 21, 2012.
41. Gamblin, A.L., Brennan, M.A., Renaud, A., and Yagita, H. Biomaterials bone tissue formation with human mesenchymal stem cells and biphasic calcium phosphate ceramics: the local implication of osteoclasts and macrophages. Biomaterials **35,** 9660, 2014.
42. Bhat, A., Hoch, A.I., Decaris, M.L., and Leach, J.K. Alginate hydrogels containing cell-interactive beads for bone formation. FASEB J **27,** 4844, 2013.
43. Jiang, T., Nukavarapu, S.P., Deng, M., Jabbarzadeh, E., Kofron, M.D., Doty, S.B., et al. Chitosan-poly(lactide-co-glycolide) microsphere-based scaffolds for bone tissue engineering: in vitro degradation and in vivo bone regeneration studies. Acta Biomater **6,** 3457, 2010.
44. Kacena, M.A., Troianao, N.W., Wilson, K.M., Coady, C.E., and Horowitz, M.C. Evaluation of two different methylmethacrylate processing, infiltration, and embedding techniques on the histological, histochemical, and immunohistochemical analysis of murine bone specimens. J Histotechnol **27,** 119, 2004.
45. Tinsley, B.A., Dukas, A., Pensak, M.J., Adams, D.J., Tang, A.H., Ominsky, M.S., Ke, H.Z., and Liberman, J.R. Systemic administration of sclerostin antibody enhances bone morphogenic protein-induced femoral defect repair in a rat model. J Bone Joint Surg Am **97,** 1852, 2015.
46. Santos, M.I., and Reis, R.L. Vascularization in bone tissue engineering: physiology, current strategies, major hurdles and future challenges. Macromol Biosci **10,** 12, 2010.
47. Kim, S., and von Recum, H. Endothelial stem cells and precursors for tissue engineering: cell source, differentiation, selection, and application. Tissue Eng Part B Rev **14,** 133, 2008.
48. Au, P., Daheron, L.M., Duda, D.G., Cohen, K.S., Tyrrell, J.A., Ryan, M., et al. Differential in vivo potential of endothelial progenitor cells from human umbilical cord blood and adult peripheral blood to form functional long-lasting vessels. Blood **111,** 1302, 2012.
49. Ingram, D.A., Mead, L.E., Tanaka, H., Meade, V., Fenoglio, A., et al. Identification of a novel hierarchy of endothelial progenitor cells using human peripheral and umbilical cord blood. Blood **104,** 2752, 2004.
50. Fedorovich, N.E., Haverslag, R.T., Dhert, W.J., and Alblas, J. The role of endothelial progenitor cells in prevascularized bone tissue engineering: development of heterogeneous constructs. Tissue Eng Part A **16,** 2355, 2010.
51. Yu, H., VandeVord, P.J., Gong, W., Wu, B., Song, Z., Matthew, H.W., et al. Promotion of osteogenesis in tissue-engineered bone by pre-seeding endothelial progenitor cells-derived endothelial cells. J Orthop Res **26,** 1147, 2008.
52. Fuchs, S., Jiang, X., Schmidt, H., Dohle, E., Ghanaati, S., Orth, C., et al. Dynamic processes involved in the prevascularization of silk fibroin constructs for bone regeneration using outgrowth endothelial cells. Biomaterials **30,** 1329, 2009.

Address correspondence to:
Syam P. Nukavarapu, PhD
Department of Orthopedic Surgery
University of Connecticut Health Center
Farmington, CT 06030

E-mail: syam@uchc.ed

Received: July 1, 2015
Accepted: February 23, 2016
Online Publication Date: March 21, 2016